

A_{FB}^t Meets LHC

JoAnne L. Hewett,¹ Jessie Shelton,² Michael
Spannowsky,³ Tim M.P. Tait,⁴ and Michihisa Takeuchi⁵

¹*SLAC National Accelerator Laboratory,
2575 Sand Hill Road, Menlo Park, CA 94025, USA*

²*Department of Physics, Yale University, New Haven, CT 06511, USA*

³*Institute of Theoretical Science, University of Oregon, Eugene, OR 97403-5203, USA*

⁴*Department of Physics and Astronomy,
University of California, Irvine, CA 92697, USA*

⁵*Institut für Theoretische Physik, Universität Heidelberg, Germany*

Abstract

The recent Tevatron measurement of the forward-backward asymmetry of the top quark shows an intriguing discrepancy with Standard Model expectations, particularly at large $t\bar{t}$ invariant masses. Measurements of this quantity are subtle at the LHC, due to its pp initial state, however, one can define a forward-central-charge asymmetry which captures the physics. We study the capability of the LHC to measure this asymmetry and find that within the SM a measurement at the 5σ level is possible with roughly 60 fb^{-1} at $\sqrt{s} = 14 \text{ TeV}$. If nature realizes a model which enhances the asymmetry (as is necessary to explain the Tevatron measurements), a significant difference from zero can be observed much earlier, perhaps even during early LHC running at $\sqrt{s} = 7 \text{ TeV}$. We further explore the capabilities of the 7 TeV LHC to discover resonances or contact interactions which modify the $t\bar{t}$ invariant mass distribution using recent boosted top tagging techniques. We find that TeV-scale color octet resonances can be discovered, even with small coupling strengths and that contact interactions can be probed at scales exceeding 6 TeV. Overall, the LHC has good potential to clarify the situation with regards to the Tevatron forward-backward measurement.

I. INTRODUCTION

The top quark, with its large mass, represents a perfect laboratory to probe electroweak symmetry breaking and its associated new physics. The Tevatron program has produced thousands of top quarks and overall observes good agreement between measured top properties and the expectations of the Standard Model (SM). As the LHC accumulates luminosity, there is potential to study the top in a whole new energy regime, perhaps revealing secrets that are too subtle to discern at lower energies.

One particular measurement at the Tevatron already shows an intriguing deviation from the SM expectation, the top-quark forward-backward asymmetry A_{FB}^t . This observable measures the tendency of the top quark in a $t\bar{t}$ pair to move forward along the same direction as the incoming quark as opposed to backward in the direction of the incoming anti-quark. In the Standard Model, this quantity deviates from zero at next-to-leading order (NLO) in QCD, and thus can be a sensitive probe of new physics which contributes in principle at tree level. Previous measurements by both CDF and D0 showed a tantalizing (but not very significant) discrepancy with the SM expectation [1–3]. The situation has become even more fascinating with the recent CDF study based on larger statistics and examining separately the high and low $t\bar{t}$ invariant mass ($M_{t\bar{t}}$) regions [4]. At low invariant masses, the asymmetry is roughly consistent with the Standard Model expectations. At high invariant masses $M_{t\bar{t}} > 450$ GeV, where one might naturally expect the effects of heavy new physics to manifest, the asymmetry is observed to be nearly 50%, exceeding the SM prediction by 3.4σ .

This result is striking, and emphasizes the need to better understand the top forward-backward asymmetry within the SM, to explore models of physics beyond the Standard Model (BSM) that could potentially explain the Tevatron measurements, and for further experimental data. In particular, the LHC is a natural place to explore high energy top physics, and could potentially provide very instructive data. However, the measurement of A_{FB}^t is somewhat subtle at the LHC, because its charge-symmetric pp initial state does not provide an automatic bias on the initial state partons participating in the reaction. Indeed, for the typical gg initial state mainly responsible for $t\bar{t}$ production at the LHC, there is no asymmetry at all. One is thus forced to rely on the subdominant $q\bar{q}$ and qg initial states, making use of the strong correlation between the rapidity of the $t\bar{t}$ system and the

direction of the incoming quark. Event-by-event, a positive forward-backward asymmetry in $q\bar{q}(qg) \rightarrow t\bar{t} + X$ translates into a positive charge asymmetry in the forward regions $|y| > y_0$ [5, 6]. This *forward-central* charge asymmetry is (assuming CP conservation) a natural LHC observable.¹

We will study the LHC prospects for measuring this top forward-central charge asymmetry, for both SM and BSM theories designed to explain the Tevatron measurement. We will see that 60 fb^{-1} at 14 TeV will allow for the small SM asymmetry to be observed, while larger asymmetries from models of new physics could be measured much sooner with tens of fb^{-1} at 7 TeV.

Ultimately, models which aim to explain the Tevatron measurements [11–24] may manifest themselves in a variety of ways at the LHC. In addition to modifications of A_{FB}^t , virtually all of the candidate theories result in an increase in $t\bar{t}$ production at large invariant mass, $M_{t\bar{t}}$, and the differential cross section $d\sigma_{t\bar{t}}/dM_{t\bar{t}}$ can be a sensitive discriminant between various models [25–27]. In fact, the unprecedented kinematic reach afforded by the LHC may allow production of new states which could contribute only virtually to Tevatron processes, revealing new $t\bar{t}$ resonances. To this end, we investigate the LHC sensitivity to both resonant and non-resonant modification of the $t\bar{t}$ invariant mass spectrum.²

The organization of this paper is as follows. In section II, we introduce a statistically stable definition of the integrated forward-central charge asymmetry and study the LHC sensitivity at $\sqrt{s} = 7$ and 14 TeV. In sections III and IV, we consider search prospects for resonances and contact operations in early LHC data. Section V contains our conclusions.

II. MEASURING A_{FB}^t AT THE LHC

As mentioned above, the forward-central charge asymmetry is a natural LHC observable probing the forward-backward asymmetry in $t\bar{t}$ pair production. It proceeds by dividing top (and anti-top) quarks based on their rapidities y between central and forward regions of the detector. The division in rapidity, y_0 defines the forward $|y| > y_0$ and central $|y| < y_0$ regions, and can be chosen to provide optimum sensitivity to the asymmetry.

¹ There have been several other recent proposals for interesting related observables [6–10].

² Some models may also produce even more unusual signals of top physics such as same sign tops [28] and resonances decaying into a top quark and a light unflavored jet [29].

For a given y_0 , we define both a forward charge asymmetry,

$$\mathcal{A}_F(y_0) = \frac{N_t(y_0 < |y| < 2.5) - N_{\bar{t}}(y_0 < |y| < 2.5)}{N_t(y_0 < |y| < 2.5) + N_{\bar{t}}(y_0 < |y| < 2.5)}, \quad (1)$$

and a central charge asymmetry,

$$\mathcal{A}_C(y_0) = \frac{N_t(|y| < y_0) - N_{\bar{t}}(|y| < y_0)}{N_t(|y| < y_0) + N_{\bar{t}}(|y| < y_0)}. \quad (2)$$

Both definitions exploit the fact that the quark parton distribution functions (PDF) have more support at large parton x than either the gluon or anti-quark PDFs, resulting in an event-by-event correlation between the rapidity of the $t\bar{t}$ pair and the incoming quark direction. As a result, a positive forward-backward asymmetry implies that the number of anti-top quarks in the central region is larger than the the number of top quarks, while the total number of top and anti-top quarks integrated over the whole rapidity region is the same (up to finite η acceptance, which we find to be a negligibly small effect). Thus, \mathcal{A}_F and \mathcal{A}_C will have opposite signs. Note that in a given event both the top and the anti-top can be either central or forward; with the definitions of Eq.(1) and Eq.(2), a single event can thus contribute to both \mathcal{A}_F and \mathcal{A}_C , and the two observables are not independent. Since the central region contains a larger proportion of symmetric gg initiated $t\bar{t}$ events, the forward charge asymmetry $\mathcal{A}_F(y_0)$ is a more sensitive probe of the underlying asymmetry in the $t\bar{t}$ cross-section.

To estimate the potential to measure a charge asymmetry with a specific significance we define the significance of an asymmetry observable as,

$$\sigma_{\mathcal{A}}(y) = \frac{|\mathcal{A}(y)|}{\Delta\mathcal{A}(y)}, \quad (3)$$

where $\Delta\mathcal{A}(y)$ is the statistical uncertainty on $\mathcal{A}(y)$

$$\Delta\mathcal{A}(y) = \frac{\sqrt{[\Delta N_t]^2 + [\Delta N_{\bar{t}}]^2}}{N_t + N_{\bar{t}}}. \quad (4)$$

In this study we confine ourselves to estimates including statistical uncertainties. Systematics may prove important as well, but require detailed detector simulations which are beyond the scope of this work.

A. Simulations

To generate the Standard Model signal we use MC@NLO [30] and shower those events with Herwig. We normalize the $t\bar{t}$ production cross section for $\sqrt{s} = 14$ TeV to its SM NNLO

rate, $\sigma_{14 \text{ TeV, NNLO}} = 918 \text{ pb}$ [31] and for $\sqrt{s} = 7 \text{ TeV}$ to the NLO cross-section obtained from MC@NLO, $\sigma_{7 \text{ TeV, NLO}} = 150 \text{ pb}$. After the selection cuts described below, the only major background is $W + \text{jets}$, which we generate using Alpgen [32], applying the MLM matching procedure for up to 5 jets [33]. CTEQ6M PDFs [34] are used for the NLO SM processes.

As a representative BSM model which can explain the Tevatron measurement of the forward-backward asymmetry, we choose the flavor-violating Z' model of [11] at its “best fit” parameters of $\alpha_X = 0.024$ and $M_{Z'} = 160 \text{ GeV}$. While this is just one model capable of explaining the Tevatron measurement, and its LHC predictions are not particularly representative of the range of possibilities, it does provide a well-motivated example for how the asymmetry could turn out at the LHC if the current Tevatron measurements are in fact the result of physics beyond the Standard Model. We generate $t\bar{t}$ production in this model at leading order using MadEvent [35] (with CTEQ6L PDFs) showered using Pythia [36]. It is worth mentioning that should this model actually turn out to be realized, there will be like-sign top and resonances decaying into a top and a light quark which may be observable with smaller data sets than will be necessary to measure a significant asymmetry at the LHC [11, 28, 29].

B. Analysis

Our analysis looks for $t\bar{t}$ where one top decays semi-leptonically (allowing a determination of the parent top charge) and the other hadronically. These “lepton + jets” events strike a balance between the desire to identify the charge of the top through its leptonic decay with a larger branching ratio and thus better statistics on the measurement from the hadronically decaying top. We proceed by selecting events with exactly one isolated lepton with $p_T > 15 \text{ GeV}$ and $|y| < 2.5$. A lepton is considered isolated provided the hadronic transverse energy E_T in a cone of $R = 0.3$ around the lepton is less than 30% of the lepton’s transverse energy $E_{T,l}$, i.e. $E_T/E_{T,l} < 0.3$.

A non-zero asymmetry is entirely the result of $q\bar{q}$ and qg initial states, and it is desirable to impose cuts which select these compared to the dominant gg initial state (which exhibits no asymmetry, and thus washes out the measurement). The fact that the valence quark PDFs have larger support at large parton x than the gluon PDF proves to be useful. Requiring large $t\bar{t}$ invariant mass results in a sample with a relatively greater proportion of $q\bar{q}$

and qg initial states, and thus a larger charge asymmetry. We enforce large $M_{t\bar{t}}$ by requiring the tops to have large transverse momentum. This has the drawback of reducing the acceptance, and smaller statistics available for the measurement. However, this price is offset by the fact that tops at moderate boost ($p_T \gtrsim m_t$) allow for cleaner event reconstruction. In particular, combinatoric backgrounds are reduced, improving the reconstruction of the parent top rapidity. Modestly boosted tops also offer improvements in b -tagging efficiency and acceptance of daughter W bosons. Such modestly boosted (hadronically decaying) top quarks are well suited for reconstruction using the HEPTopTagger, which is designed to operate on tops with $p_T \gtrsim 200$ GeV [37, 38].

After removing the isolated lepton, we group all remaining visible particles into massless cells of size $\Delta\eta \times \Delta\phi = 0.1 \times 0.1$. Cells with transverse energy above 0.5 GeV are retained for jet clustering. Initially, the event is clustered (using FastJet [39]) according to the Cambridge-Aachen jet-finding algorithm [40] with a large effective cone size $R = 1.5$. We require that the hardest jet have transverse momentum larger than $p_{T,\min} > 200$ GeV; we will refer to this jet as the “fat jet”. Harder p_T cuts result in too much loss of acceptance and ultimately reduce sensitivity to the asymmetry. We require this jet to be tagged as a top candidate by the HEPTopTagger [37, 38]. To suppress the W +jets background we additionally require one b -tag in the fat jet, for which we assume a 60% tagging efficiency and a 2% fake rate. Note that at the LHC the W +jets background produces more positively charged leptons than negatively charged leptons. This can fake a bigger positive charge asymmetry than produced from the SM $t\bar{t}$ process alone, and it is critical to reduce this background in order to accurately determine the top charge asymmetry. After requiring the hadronic top to be reconstructed using the HEPTopTagger and demanding the b tag, we find that the W + jets background becomes irrelevant, see Table I.

The asymmetries of Eq.(1) and Eq.(2) depend on the rapidity of the leptonic top as well. Several approaches have been proposed for this purpose [41, 42]. Here we take the simple approach of identifying the leptonic top rapidity with the lepton rapidity. The degree of the correlation of the lepton rapidity with that of its parent top depends to some degree on the top polarization [43] and in principle one could recover additional information from a more careful treatment of the semileptonic top. While the degree of polarization increases with increasing boost, so does the kinematic correlation of the lepton rapidity with the top rapidity. In our present study, as we have not retained polarization information in

modeling the top decays, the lepton rapidity provides a good approximation to the top rapidity regardless of the production mechanism.

A further cut can improve the statistical significance of the asymmetry. After identifying the region with optimal \mathcal{A}_F and \mathcal{A}_C we veto events where both tops are either forward or central. Those events do not contribute to the asymmetry. Although this cut results only in a small increase of the statistical significance to extract the forward asymmetry \mathcal{A}_F , it is very effective in removing symmetric gluon-gluon initial states. Thus, by definition, \mathcal{A}_F and \mathcal{A}_C contain the same information and become equally significant.

C. Results

Our results are summarized in Figure 1 and in Tables I and II. Figure 1 shows the asymmetry and its significance as a function of y_0 for both the SM and Z' models. As expected, \mathcal{A}_F is more sensitive than \mathcal{A}_C . We find that an optimum choice for the separation parameter is $y_0 \sim 1.5$, which we adopt in deriving the numbers in the tables. Tables I ($\sqrt{s} = 14$ TeV) and II ($\sqrt{s} = 7$ TeV), show the number of events per fb^{-1} , resulting $\mathcal{A}_{F,C}$ for 25 (10) fb^{-1} , and the statistical significance as defined in Eq. (3) of the deviation of \mathcal{A} from zero for both the SM and our reference Z' model.

We conclude that the SM forward charge asymmetry can reach the 5σ level at the LHC with $\sqrt{s} = 14$ TeV after about 60 fb^{-1} . If the charge asymmetry is larger, compatible with the effect measured by CDF, the asymmetry can usually be extracted much earlier. For the Z' model introduced in [11] a 5σ discovery can be achieved after less than 2 fb^{-1} . With early data at $\sqrt{s} = 7$ TeV it will be challenging to extract the charge asymmetry reliably. $2 - 3\sigma$ evidence might be observable after 10 fb^{-1} , yielding 2σ at 5 fb^{-1} if it is enhanced by new physics, but the SM asymmetry cannot be reconstructed from early data using boosted top quarks. If we require for the accepted events that one of the tops has to be in the central region and one in the forward region, where $|y| = 1.5$ discriminates between those two regions, we find a small increase of the statistical significance for all of the scenarios. After 25 fb^{-1} at $\sqrt{s} = 14$ TeV we find for the SM asymmetry 3.65σ and for the Z' model 20.9σ . At $\sqrt{s} = 7$ TeV with 10 fb^{-1} we find for the SM 0.38σ and for the Z' model 3.0σ . It would be interesting to try top reconstruction methods which are effective at lower p_T [44, 45], but such studies are beyond the scope of this work.

		$(N_+ + N_-), (N_+ - N_-), \Delta N$			$\mathcal{A}_{(F,C)25\text{fb}^{-1}}$	$\sigma_{25\text{fb}^{-1}}$
$t\bar{t}$ (SM 14 TeV)	$0 < y < 2.5$	10350	0			
	$1.5 < y < 2.5$	1869	27.8	43.2	0.0149 ± 0.0046	3.24
	$0 < y < 1.5$	8481	-27.8	92.1	-0.0033 ± 0.0022	1.51
$t\bar{t}$ (BSM 14 TeV)	$0 < y < 2.5$	9153	0			
	$1.5 < y < 2.5$	1695	151.3	41.2	0.0893 ± 0.0049	18.3
	$0 < y < 1.5$	7458	-151.3	86.4	-0.0203 ± 0.0023	8.76
W +jets (SM 14 TeV)	$0 < y < 2.5$	20.88	0			
	$1.5 < y < 2.5$	5.54	0.46	2.35	-	-
	$0 < y < 1.5$	15.34	-0.46	3.92	-	-

TABLE I: Expected number of events after an integrated luminosity of 1 fb^{-1} at $\sqrt{s} = 14 \text{ TeV}$. The total cross section is normalized to 918pb (NNLO). We give the error for the resulting asymmetry and its significance, σ , for 25 fb^{-1} .

		$(N_+ + N_-), (N_+ - N_-), \Delta N$			$\mathcal{A}_{(F,C)10\text{fb}^{-1}}$	$\sigma_{10\text{fb}^{-1}}$
$t\bar{t}$ (SM 7 TeV)	$0 < y < 2.5$	1390.9	0			
	$1.5 < y < 2.5$	163.8	1.43	12.8	0.0087 ± 0.025	0.35
	$0 < y < 1.5$	1227.1	-1.43	35.0	-0.0012 ± 0.0090	0.13
$t\bar{t}$ (BSM 7 TeV)	$0 < y < 2.5$	1194.8	0			
	$1.5 < y < 2.5$	140.3	10.55	11.8	0.075 ± 0.027	2.81
	$0 < y < 1.5$	1054.5	-10.55	32.5	-0.010 ± 0.0097	1.03

TABLE II: Expected number of events after an integrated luminosity of 1 fb^{-1} . The total cross section is normalized to 150 pb (NLO). We give the error for the resulting asymmetry and its significance, σ , for 10 fb^{-1} .

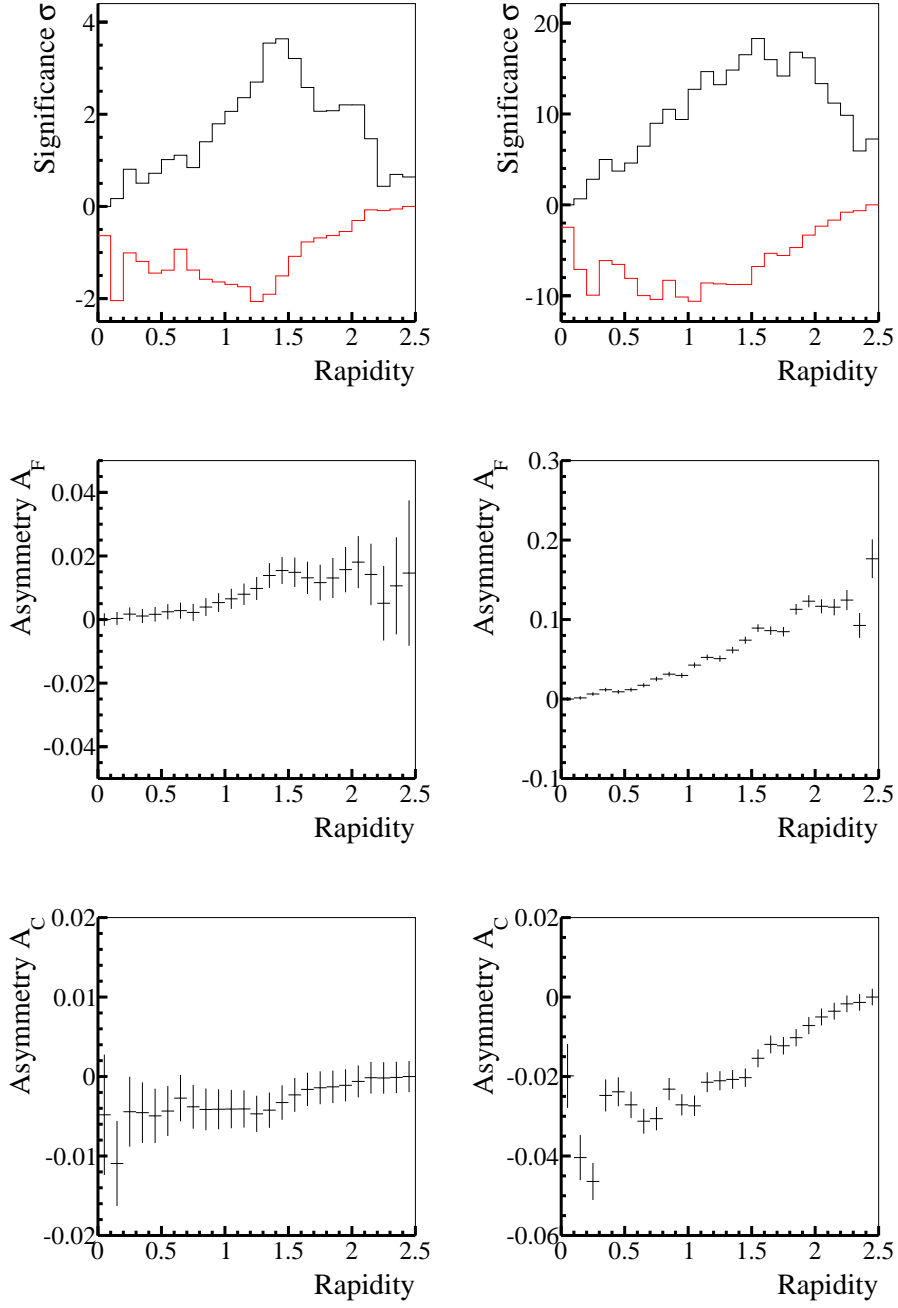


FIG. 1: The upper panels show the asymmetry significance of Eq.(3) as a function of y_0 , for $\mathcal{A}_F(y_0)$ (black) and $\mathcal{A}_C(y_0)$ (red). The left plot shows results for the SM and the right plot for the Z' model described in the text. The middle panels show $\mathcal{A}_F(y_0)$ for SM (left) and BSM (right) as a function of y_0 including statistical error bars. The lower panels show $\mathcal{A}_C(y_0)$ for SM (left) and BSM (right) as a function of y_0 including statistical error bars.

III. RESONANCES

While the top-quark forward-central asymmetry will take significant integrated luminosity to detect, new physics in the top invariant mass spectrum can be observed in the early phases of LHC running with center-of-mass energies of 7 TeV. The intermediate mass range, $1 \text{ TeV} \lesssim M_{t\bar{t}} \lesssim 2 \text{ TeV}$, is of special interest, both because the LHC will be able to quickly probe this region, and because the Tevatron anomaly suggests it is a prime spot for new physics to appear. This intermediate mass range is also a particularly interesting kinematic environment. Top-quark pairs with invariant mass in this range will typically have some, but not all, of their decay products merging in the detector. To fully utilize the events in this range, it is necessary to use techniques that interpolate between traditional top reconstruction methods using isolated jets and leptons [46], and new approaches designed to tag the top as a single object (see [47] for a recent review). The ultimate performance of these new reconstruction techniques is still to be validated, and here we focus on obtaining representative estimates of sensitivity to the production of new resonances in the $t\bar{t}$ channel, rather than on furthering the tagging state-of-the-art.

We compute the resonance search reach for various generic models using the semileptonic channel resulting from top-quark pair production. We adopt the top tagger described in [48], which is based on the work in Refs. [49, 50]. The baseline version of this tagging technique yields the best efficiency at lower top-quark momentum and we thus employ that version here. This reconstruction technique has been specifically designed for top-quarks produced with moderate boost, $p_T \gtrsim 200 \text{ GeV}$, and remains viable for values of the top transverse momentum up to the TeV range. Using the results in [48], we find that the tagging efficiency lies in the range 5 – 10% for $900 \lesssim M_{t\bar{t}} \lesssim 2500 \text{ GeV}$, where this figure includes the top-quark pair branching fraction into e, μ semileptonic states. This efficiency is indeed remarkably improved over that from traditional tagging techniques [46] (which are of order 1%, including the semi-leptonic branching fraction). However, we note that for lower values of $M_{t\bar{t}}$, the transitional reconstruction techniques employed here become inefficient. Additional sensitivity to resonance production in this range could be gained by supplementing these techniques with traditional reconstruction methods.

We focus on the production of color-octet and color-singlet vector resonances, noting that the color-octet case is a candidate that generates [12, 25] the observed top-quark forward-

backward asymmetry at the Tevatron. The reconstruction techniques described above were developed for vector exchange contributions to top pair production, and some modification would be required to account for the different acceptances associated with scalar and tensor resonances. Vector resonance production proceeds solely through s -channel exchange in $q\bar{q}$ annihilation. Contributions from gluon-gluon initial states do not occur at tree level, with renormalizable interactions being excluded by gauge invariance. For example, a color octet vector resonance occurs in models with extra spatial dimensions as a Kaluza-Klein mode of the gluon itself. However, orthonormality of the wave functions results in the g - g - g_{KK} coupling (where g_{KK} is a gluon Kaluza Klein state) being zero [51].

The production cross section for s -channel vector exchange in $q\bar{q} \rightarrow t\bar{t}$ can be written most generally as [52]

$$\frac{d\sigma}{d\cos\theta} = \frac{\pi\alpha_{(s,em)}}{2} \hat{s} C_F \beta \sum_{i,j} P_{ij}^{ss} \left[B_{ij}(1 + \beta^2 \cos^2\theta) + 2C_{ij}\beta \cos\theta + E_{ij}(1 - \beta^2) \right], \quad (5)$$

where the sum extends over all vector bosons being exchanged. Here, we have defined

$$\begin{aligned} B_{ij} &= (v_i v_j + a_i a_j)_q (v_i v_j + a_i a_j)_t, \\ C_{ij} &= (v_i a_j + a_i v_j)_q (v_i a_j + a_i v_j)_t, \\ E_{ij} &= (v_i v_j + a_i a_j)_q (v_i v_j - a_i a_j)_t, \\ P_{ij}^{ss} &= \frac{(\hat{s} - M_i^2)(\hat{s} - M_j^2) + (\Gamma_i M_i)(\Gamma_j M_j)}{[(\hat{s} - M_i^2)^2 + (\Gamma_i M_i)^2][(\hat{s} - M_j^2)^2 + (\Gamma_j M_j)^2]}, \end{aligned} \quad (6)$$

with the couplings being normalized as $g_i \bar{f} \gamma_\mu (v_i^f - a_i^f \gamma_5) f V_i^\mu$, $\beta^2 = (1 - 4m_t^2/\hat{s})$ and C_F is the usual color factor. In what follows, we examine the cases of a color-octet resonance with either pure vector or axial couplings, as well as a color-singlet boson with v^f, a^f being identical to those of the SM Z boson. We vary the overall coupling strength and compute the width for each case. We assume that no new exotic decay channels contribute to the width.

Figure 2 displays the top-quark pair invariant mass distribution for both a color-octet and color-singlet resonance with mass of 1 TeV, as well as for the SM. The resonance couplings are taken to be SM strength, *i.e.*, g_s and g_{wk} , respectively. The couplings for the color-octet vector resonance are taken to be purely axial-vector, while those for the color-singlet are taken to be the same as for the SM Z boson. The top (bottom) set of curves give the event rate without (with) including the tagging efficiency. The jagged curves at low invariant mass

reflect the interference between the inefficiency of the tagging routine at lower values of the top-quark p_T and the falling production cross section. This figure demonstrates that for $M_{t\bar{t}} \gtrsim 900$ GeV, the tagging efficiencies have indeed reached their nominal value of 5 – 10% stated above.³ We see that for the color-octet state, the resonance is easily observable above the SM background. However, it is clear that the resonance peak is much smaller for the color-singlet vector boson, and hence we expect a reduced sensitivity in this case.

The recent ATLAS study [48] demonstrated that the main source of background for resonances in the $t\bar{t}$ semi-leptonic channel arise from SM top production itself, while reducible backgrounds, such as W +jets, are negligible in the $M_{t\bar{t}}$ range of interest here. Systematic errors arise from uncertainties in the NLO $t\bar{t}$ cross section and the parton distribution functions; we estimate that these combined errors are of order 50% at high invariant masses [53]. For our discovery criteria, we require $S/\sqrt{B} \geq 5$ in the $M_{t\bar{t}}$ region that is within 10% of the resonance mass on either side of the resonance peak, *i.e.*, $\Delta M_{t\bar{t}} = M_V \pm 0.1M_V$. We include statistical as well as the 50% theoretical systematic errors.

The discovery reach for a color-octet vector resonance is shown in Fig. 3 in the coupling strength - mass plane for both 1 and 5 fb⁻¹ of integrated luminosity at the 7 TeV LHC. Here, we have assumed either purely vector or purely axial vector couplings and taken $g_{SM} = g_s$. We see that the reach is equivalent for both types of couplings. We see that for large couplings, the mass reach saturates at values of $\sim 2.1(2.5)$ TeV for the two integrated luminosities. For smaller values of the couplings, we see that the production cross section becomes too small to be observed once the coupling is roughly 40-50% SM strength. For this region, the use of traditional top tagging techniques may enhance the discovery reach. The corresponding discovery reach for color-singlet vector resonances with SM-like couplings are given in Table III for several values of the coupling strength. Here, we see that the coupling must be roughly of order SM strength, or higher, in order for the resonance to be observed. These results mirror that from dijet resonance searches [54].

We briefly note that in principle color-octet scalar resonances, as well as Kaluza Klein Graviton production in models with warped extra dimensions [55], can also be observed in the $t\bar{t}$ invariant mass spectrum. Most models with a heavy scalar boson predict $q\bar{q}S$ couplings that are proportional to m_q and hence s -channel production proceeds mainly

³ We note that the tagging efficiencies are computed for a $M_{t\bar{t}}$ bin size of 100 GeV.

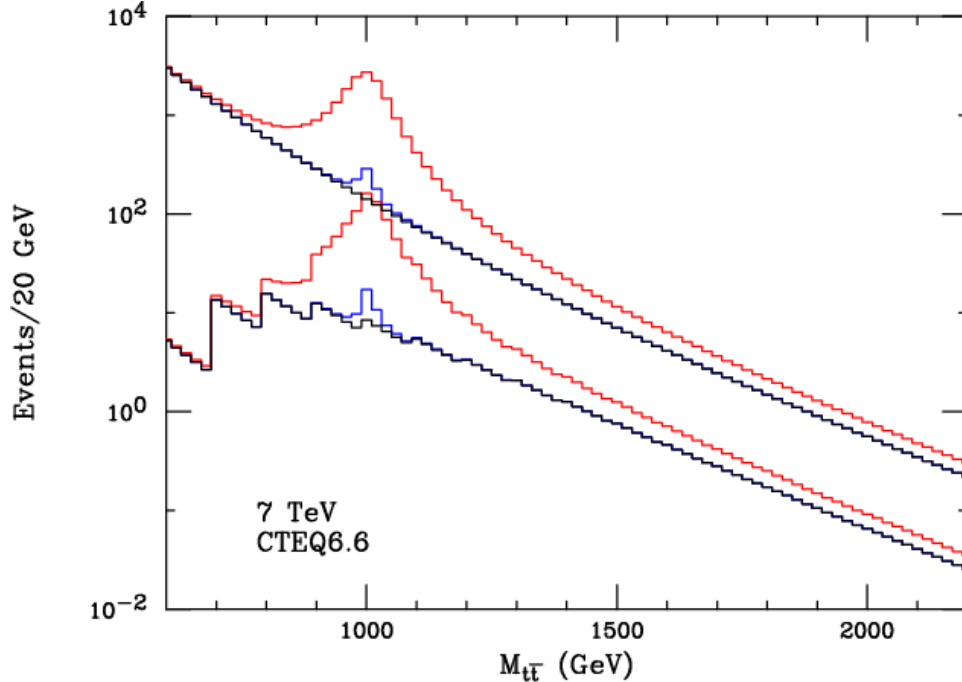


FIG. 2: Top-quark pair invariant mass spectrum including a color-octet (red) and color-singlet (blue) vector exchange with couplings as described in the text. The SM distribution is represented by the black curves. The bottom (top) set of curves include (are without) the semi-leptonic tagging efficiency.

g/g_{wk}	1 fb^{-1}	5 fb^{-1}
1.8	1.50 (1.58)	1.92 (2.00)
2.0	1.76 (1.82)	2.16 (2.18)
2.5	1.94 (2.02)	2.34 (2.42)
3.0	2.12 (2.16)	2.52 (2.56)

TABLE III: Discovery reach in TeV for a color-singlet vector resonance with coupling structure identical to the SM Z boson for various coupling strengths relative to g_{wk} for 1 and 5 fb^{-1} of integrated luminosity. The numbers outside (within) the parenthesis correspond to the semi-leptonic (semi-leptonic and hadronic) channel.

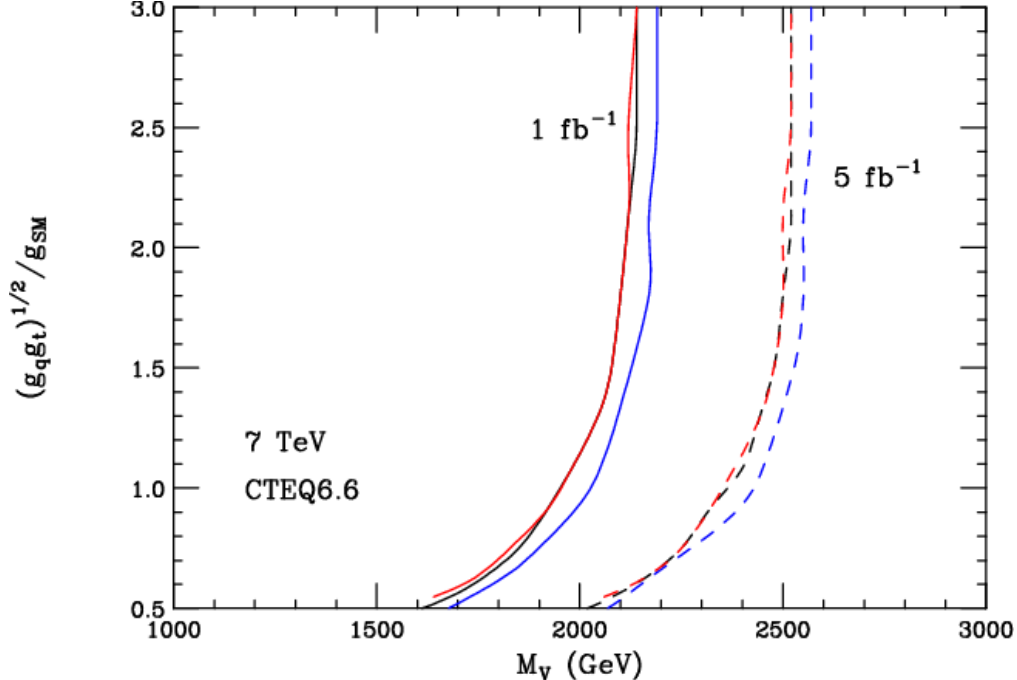


FIG. 3: Discovery reach in the coupling strength-mass plane for purely vector (axial) coupled color-octet vector resonances corresponding to the black (red) curves for the integrated luminosities as indicated for the semi-leptonic channel. The blue curves show the increase in discovery reach when the hadronic channel is also included.

through a highly model-dependent loop level ggS 3-point function. In addition, sizeable cross sections can be obtained in models with warped extra dimensions via $gg \rightarrow G_{KK} \rightarrow t\bar{t}$ (where G_{KK} is a Kaluza-Klein graviton state), however the production rates are highly dependent on the placement of the fermions in the extra-dimensional bulk.

In order to increase event statistics, one could also include the full hadronic channel; we provide a quick estimate of how this modifies the discovery reach here. In this channel we employ the HEPTopTagger of [37, 38] discussed at length in the previous section. We find that the tagging efficiency lies in the range 2 – 4% for the $M_{t\bar{t}}$ region of interest to us here, where this value includes the top-quark pair hadronic branching fraction. An important background in this channel arises from QCD dijet production. Requiring two subjets inside the tagged fat jets to be tagged as b -quarks gives a dominant background from bottom pair production. For the HEPTopTagger, the probability for a QCD jet with $p_T > 200$ GeV to be tagged as a top is approximately 2-3%. We roughly estimate the QCD background using Madgraph to compute the leading order bottom pair production cross-section, then

imposing a 0.6 b -tagging efficiency and a 2% top mistag probability. This suppresses the QCD background beneath the dominant background of standard model top production. The resulting effect on the discovery reach by including the hadronic channel is represented in Fig. 3 by the blue curves and in Table III by the numbers given in parenthesis. We see that adding this channel increases the reach by roughly 100 GeV, indicating that this resonance search is becoming limited by the kinematics of the parton distribution functions.

IV. CONTACT OPERATORS

The top-quark pair invariant mass distribution also provides constraints on models which can generate a large forward-backward asymmetry in the absence of a narrow resonance. In particular, broad resonances with large couplings can easily generate [25] the magnitude of the effect observed at the Tevatron. Such non-resonant contributions to top pair production can yield significant deviations in the invariant mass spectrum at large values of $M_{t\bar{t}}$.

Numerous forms of contact operators can affect $t\bar{t}$ pair production at the LHC [56–59]. Here, we focus on a limited subset that can potentially contribute to an angular $t\bar{t}$ asymmetry. In particular, such operators must be able to interfere with the $q\bar{q}$ -initiated scattering process and thus we turn our attention to the usual four-quark operators. Requiring further that the operators interfere with the dominant QCD production amplitude, without chiral suppression from the light quark masses, identifies the following set of operators of interest:

$$\mathcal{O}_{(L/R)(L/R)} = \frac{g_{eff}^2 \eta}{2\Lambda^2} (\bar{q}^a \gamma^\mu q^b)_{L/R} (\bar{t}^b \gamma_\mu t^a)_{L/R}, \quad (7)$$

where the light quark flavor indices have been suppressed, a, b represent color indices, $\eta = \pm 1$, and the subscript L/R indicates that the current structure within each parenthesis can be either left- or right-handed. Various possible choices of the chiralities lead to different predictions for the angular distributions for $t\bar{t}$ production. It is conventional to define $g_{eff}^2 = 4\pi$ since the binding force is strong when Q^2 approaches the cut-off Λ^2 .

At the same order in $1/\Lambda$, $t\bar{t}$ production also receives contributions from two additional operators which modify the $t\bar{t}$ - g interaction. The chromo-magnetic operator $m_t G_{\mu\nu}^a \bar{t} \sigma^{\mu\nu} \lambda^a t$ also interferes with the SM $q\bar{q} \rightarrow t\bar{t}$ production amplitude, and can affect the $t\bar{t}$ production rate [60], but does not contribute to the asymmetry and thus we do not consider it further. The operator $G_{\mu\nu}^a \bar{t} \gamma^\mu \lambda^a D^\nu P_R t$ can be rewritten using the equations of motion in terms of a

vector-like, flavor-universal four-quark operator included in Eq. (7) [57, 59].

Interference between the contact terms and the usual gauge interactions can lead to observable deviations from SM predictions at energies lower than the scale Λ . Summing over the light-quark flavors, we find the following spin and color averaged matrix element for the operators $\mathcal{O}_{LL,RR}$,

$$|\bar{\mathcal{M}}|^2 = \frac{4\pi\eta g_s^2}{9\Lambda^2 s} \left(\frac{4m^2}{s} + \frac{4(u - m^2)^2}{s^2} \right) \quad (8)$$

and the corresponding contribution to the interference term with the SM is

$$\frac{d\sigma}{d\cos\theta} = \frac{\alpha_s\beta}{9s} \frac{\pi\eta}{2\Lambda^2} \left(\frac{4m^2}{s} + 1 + \beta\cos\theta + \beta^2\cos^2\theta \right). \quad (9)$$

For $\mathcal{O}_{LR,RL}$, the averaged matrix element is

$$|\bar{\mathcal{M}}|^2 = \frac{4\pi\eta g_s^2}{9\Lambda^2 s} \left(\frac{4m^2}{s} + \frac{4(t - m^2)^2}{s^2} \right) \quad (10)$$

giving

$$\frac{d\sigma}{d\cos\theta} = \frac{\alpha_s\beta}{9s} \frac{\pi\eta}{2\Lambda^2} \left(\frac{4m^2}{s} + 1 - \beta\cos\theta + \beta^2\cos^2\theta \right). \quad (11)$$

Note that these two sets of operators only yield different results for $t\bar{t}$ angular distributions, and that after integrating over $\cos\theta$, all four operators contribute equally to the total production rate at this order in Λ .

Summing over 20 GeV bins in the $M_{t\bar{t}}$ spectrum, we employ a χ^2 distribution, evaluated as usual, to determine the 95% C.L. search reach for these operators. We use only the semi-leptonic channel with $\ell = e, \mu$ and take the tagging efficiencies as described in the previous Section III. Our results are presented in Table IV for $\eta = \pm 1$ with 1 and 5 fb⁻¹ of the integrated luminosity at 7 TeV. We see that the 7 TeV LHC has a reasonable reach in the $t\bar{t}$ channel and that there is not much difference between $\eta = \pm 1$. Observation of a signal, or not, will provide information on the discovery potential for resonance production at the higher energy 14 TeV LHC.

V. CONCLUSIONS

The LHC provides an extraordinary opportunity to study the top quark at high energies. Even modest amounts of LHC data afford a vision of the top quark which is radically different from the one provided by the Tevatron, and there is much room for discoveries

η	1 fb ⁻¹	5 fb ⁻¹
+1	3.2 (3.78)	4.8 (7.2)
-1	3.2 (3.6)	4.7 (6.0)

TABLE IV: 95% C.L. search reach in TeV for the contact interaction scale Λ with $\eta = \pm 1$ and 1 or 5 fb⁻¹ of integrated luminosity at the 7 TeV LHC. The numbers outside (within) the parenthesis correspond to the semi-leptonic (semi-leptonic and hadronic) event sample.

and surprises. In fact, the Tevatron may already be providing the first hints for what the LHC may discover through its measurement of A_{FB}^t . In this work, we have examined the prospects for several early measurements of top physics at the LHC, including remeasuring A_{FB}^t itself, and searching for anomalies in the invariant mass distribution of $t\bar{t}$ events, including resonances and contact interactions.

We have made use of the recent developments in boosted top tagging to facilitate all of these searches. Top-tagging is a powerful new tool that is ideal for measurements involving energetic top quarks – exactly the regime where early LHC data is truly probing new territory compared to the Tevatron. Since the measurement of A_{FB}^t depends crucially on assigning a direction to the top quark, boosted top reconstruction is a particularly incisive tool. Our finding is that a reasonably precise measurement of A_{FB}^t is feasible with a modest amount of data, but it is worth emphasizing that we have not fully optimized our analysis, and (particularly in light of our positive results) more sophisticated investigation involving a full detector simulation are warranted. For example, the p_T cut required for tops in the measurement of $\mathcal{A}_{\mathcal{F}}$ has not been optimized on fully showered events, as for tops with $p_T < 200$ GeV entirely different reconstruction strategies are required. Our results leave open the possibility that precise $t\bar{t}$ reconstruction combined with background rejection at low p_T could enhance prospects for measuring the asymmetry.

A recent measurement by CMS [61] takes a different approach to the top forward-backward asymmetry by measuring the asymmetry in the rapidity distributions of tops and anti-tops, $A_C^t = (|\eta_t| - |\eta_{\bar{t}}|)/(|\eta_t| + |\eta_{\bar{t}}|)$. As defined, this observable receives large contributions from the dominant $gg \rightarrow t\bar{t}$ process, yielding small values for the net asymmetry. The LHC sensitivity to predicted values of A_C^t are limited by proportionally large

systematic errors; if these errors can be reduced to the percent level, a twofold improvement over the current reported errors, then 2-3 σ sensitivity to large BSM partonic asymmetries may be possible in the TeV run, broadly comparable to our results. As our approach is statistics-limited in the early LHC run, the comparison between our results and those of CMS naturally raises the question of whether it is possible to improve sensitivity at 7 TeV with alternate reconstruction techniques.

In conclusion, we find that $\mathcal{A}_F(y)$ can provide an effective measurement of the forward-backward asymmetry of top pair production at the LHC, both in the Standard Model, as well as in models designed to explain the recent Tevatron measurements. Boosted top reconstruction proves a helpful tool. We further study the early prospects for discovery of resonances or contact interactions in $t\bar{t}$ production, and find that with small amounts of data, the LHC will extend our knowledge to a large degree. The LHC is a top quark factory, and in the next years will provide a vista of top completely unseen before now.

Acknowledgments

We gratefully acknowledge useful conversations M. Son, T. Plehn, T. Rizzo, and B. Tweedie. T. Tait is grateful to the SLAC theory group for their generosity during his many visits. The work of JH is supported by SLAC, operated by Stanford University for the US Department of Energy under contract DE-AC02-76SF00515. JS was supported in part by DOE grant DE-FG02-92ER40704, MS was supported by US Department of Energy under contract number DE-FG02-96ER40969. TMPT was supported by the NSF under grant PHY-0970171. This work was inspired in part by the workshop “The Terascale at LHC 0.5 and Tevatron” which was co-sponsored by the Universities of Washington and Oregon and supported by the DOE under contracts DE-FGO2-96-ER40956 and DE-FG02-96ER40969 .

-
- [1] V. M. Abazov *et al.* [D0 Collaboration], Phys. Rev. Lett. **100**, 142002 (2008) [arXiv:0712.0851 [hep-ex]].
- [2] T. Aaltonen *et al.* [CDF Collaboration], “Forward-Backward Asymmetry in Top Quark Production in $p\bar{p}$ Phys. Rev. Lett. **101**, 202001 (2008) [arXiv:0806.2472 [hep-ex]].

- [3] T. Aaltonen *et al.* [CDF Collaboration], “First Measurement of the $t\bar{t}$ Differential Cross Section $d\sigma/dM_{t\bar{t}}$ in $p\bar{p}$ Collisions at $\sqrt{s} = 1.96$ Phys. Rev. Lett. **102**, 222003 (2009) [arXiv:0903.2850 [hep-ex]].
- [4] T. Aaltonen *et al.* [CDF Collaboration], arXiv:1101.0034 [hep-ex].
- [5] J. H. Kuhn and G. Rodrigo, Phys. Rev. Lett. **81**, 49 (1998) [arXiv:hep-ph/9802268],
J. H. Kuhn and G. Rodrigo, Phys. Rev. D **59**, 054017 (1999) [arXiv:hep-ph/9807420].
- [6] O. Antunano, J. H. Kuhn and G. Rodrigo, Phys. Rev. D **77**, 014003 (2008) [arXiv:0709.1652 [hep-ph]].
- [7] Y. k. Wang, B. Xiao and S. h. Zhu, Phys. Rev. D **82**, 094011 (2010) [arXiv:1008.2685 [hep-ph]],
Y. k. Wang, B. Xiao and S. h. Zhu, Phys. Rev. D **83**, 015002 (2011) [arXiv:1011.1428 [hep-ph]].
- [8] B. Xiao, Y. K. Wang, Z. Q. Zhou and S. h. Zhu, arXiv:1101.2507 [hep-ph].
- [9] D. Choudhury, R. M. Godbole, S. D. Rindani, P. Saha, [arXiv:1012.4750 [hep-ph]]; D. W. Jung,
P. Ko and J. S. Lee, arXiv:1011.5976 [hep-ph].
- [10] G. Rodrigo and P. Ferrario, Nuovo Cim. C **33**, 04 (2010) [arXiv:1007.4328 [hep-ph]]; P. Ferrario
and G. Rodrigo, PoS D **IS2010**, 191 (2010) [arXiv:1006.5593 [hep-ph]]; P. Ferrario and
G. Rodrigo, J. Phys. Conf. Ser. **171**, 012091 (2009) [arXiv:0907.0096 [hep-ph]].
- [11] S. Jung, H. Murayama, A. Pierce, J. D. Wells, Phys. Rev. **D81**, 015004 (2010).
[arXiv:0907.4112 [hep-ph]].
- [12] P. H. Frampton, J. Shu, K. Wang, Phys. Lett. **B683**, 294-297 (2010). [arXiv:0911.2955 [hep-ph]].
- [13] J. Shu, T. M. P. Tait, K. Wang, Phys. Rev. **D81**, 034012 (2010). [arXiv:0911.3237 [hep-ph]];
I. Dorsner, S. Fajfer, J. F. Kamenik and N. Kosnik, Phys. Rev. D **81**, 055009 (2010)
[arXiv:0912.0972 [hep-ph]]; I. Dorsner, S. Fajfer, J. F. Kamenik and N. Kosnik, Phys. Rev. D
82, 094015 (2010) [arXiv:1007.2604 [hep-ph]].
- [14] A. Djouadi, G. Moreau, F. Richard, R. K. Singh, Phys. Rev. **D82**, 071702 (2010).
[arXiv:0906.0604 [hep-ph]].
- [15] A. Arhrib, R. Benbrik, C. -H. Chen, Phys. Rev. **D82**, 034034 (2010). [arXiv:0911.4875 [hep-ph]].
- [16] K. Cheung, W. -Y. Keung, T. -C. Yuan, Phys. Lett. **B682**, 287-290 (2009). [arXiv:0908.2589 [hep-ph]].

- [17] V. Barger, W. -Y. Keung, C. -T. Yu, Phys. Rev. **D81**, 113009 (2010). [arXiv:1002.1048 [hep-ph]].
- [18] Q. H. Cao, D. McKeen, J. L. Rosner, G. Shaughnessy and C. E. M. Wagner, Phys. Rev. D **81**, 114004 (2010) [arXiv:1003.3461 [hep-ph]]; D. W. Jung, P. Ko, J. S. Lee and S. h. Nam, Phys. Lett. B **691**, 238 (2010) [arXiv:0912.1105 [hep-ph]].
- [19] E. Alvarez, L. Da Rold, A. Szyrkman, C,” [arXiv:1011.6557 [hep-ph]].
- [20] J. Shelton, K. M. Zurek, [arXiv:1101.5392 [hep-ph]].
- [21] V. Barger, W. -Y. Keung, C. -T. Yu, [arXiv:1102.0279 [hep-ph]].
- [22] B. Grinstein, A. L. Kagan, M. Trott, J. Zupan, [arXiv:1102.3374 [hep-ph]].
- [23] K. M. Patel, P. Sharma, [arXiv:1102.4736 [hep-ph]].
- [24] G. Isidori and J. F. Kamenik, arXiv:1103.0016 [hep-ph].
- [25] Y. Bai, J. L. Hewett, J. Kaplan, T. G. Rizzo, [arXiv:1101.5203 [hep-ph]]; P. Ferrario and G. Rodrigo, JHEP **1002**, 051 (2010) [arXiv:0912.0687 [hep-ph]]; P. Ferrario and G. Rodrigo, Phys. Rev. D **78**, 094018 (2008) [arXiv:0809.3354 [hep-ph]].
- [26] B. Bhattacharjee, S. S. Biswal, D. Ghosh, [arXiv:1102.0545 [hep-ph]].
- [27] B. Xiao, Y. -k. Wang, S. -h. Zhu, Phys. Rev. **D82**, 034026 (2010). [arXiv:1006.2510 [hep-ph]]; K. Cheung and T. C. Yuan, arXiv:1101.1445 [hep-ph]; J. A. Aguilar-Saavedra, M. Perez-Victoria, [arXiv:1103.2765 [hep-ph]]; M. I. Gresham, I. -W. Kim, K. M. Zurek, [arXiv:1103.3501 [hep-ph]]; Z. Ligeti, M. Schmaltz, G. M. Tavares, [arXiv:1103.2757 [hep-ph]]; K. Blum *et al.*, arXiv:1102.3133 [hep-ph]; C. Delaunay, O. Gedalia, Y. Hochberg, G. Perez and Y. Soreq, arXiv:1103.2297 [hep-ph].
- [28] E. L. Berger, Q. H. Cao, C. R. Chen, C. S. Li and H. Zhang, arXiv:1101.5625 [hep-ph]; H. Zhang, E. L. Berger, Q. H. Cao, C. R. Chen and G. Shaughnessy, Phys. Lett. B **696**, 68 (2011) [arXiv:1009.5379 [hep-ph]]; J. Cao, L. Wang, L. Wu and J. M. Yang, arXiv:1101.4456 [hep-ph].
- [29] M. I. Gresham, I. W. Kim and K. M. Zurek, arXiv:1102.0018 [hep-ph].
- [30] S. Frixione, B. R. Webber, JHEP **0206**, 029 (2002), <https://www.hep.phy.cam.ac.uk/theory/webber/MCatNLO/> .
- [31] S. Moch and P. Uwer, Phys. Rev. D **78**, 034003 (2008) [arXiv:0804.1476 [hep-ph]].
- [32] M. L. Mangano, M. Moretti, F. Piccinini, R. Pittau, A. D. Polosa, JHEP **0307**, 001 (2003). [hep-ph/0206293].

- [33] S. Hoeche, F. Krauss, N. Lavesson, L. Lonnblad, M. Mangano, A. Schalicke, S. Schumann, [hep-ph/0602031].
- [34] P. M. Nadolsky *et al.*, Phys. Rev. D **78**, 013004 (2008) [arXiv:0802.0007 [hep-ph]].
- [35] J. Alwall, P. Demin, S. de Visscher, R. Frederix, M. Herquet, F. Maltoni, T. Plehn, D. L. Rainwater *et al.*, JHEP **0709**, 028 (2007). [arXiv:0706.2334 [hep-ph]].
- [36] T. Sjostrand, S. Mrenna and P. Z. Skands, JHEP **0605**, 026 (2006) [arXiv:hep-ph/0603175].
- [37] T. Plehn, G. P. Salam and M. Spannowsky, Phys. Rev. Lett. **104**, 111801 (2010) [arXiv:0910.5472 [hep-ph]].
- [38] T. Plehn, M. Spannowsky, M. Takeuchi and D. Zerwas, JHEP **1010**, 078 (2010) [arXiv:1006.2833 [hep-ph]].
- [39] M. Cacciari, G. P. Salam, Phys. Lett. **B641**, 57-61 (2006); M. Cacciari, G. P. Salam and G. Soyez, <http://fastjet.fr>
- [40] Y. L. Dokshitzer, G. D. Leder, S. Moretti, B. R. Webber, JHEP **9708**, 001 (1997). [hep-ph/9707323]; M. Wobisch, T. Wengler, [hep-ph/9907280].
- [41] K. Rehermann and B. Tweedie, arXiv:1007.2221 [hep-ph].
- [42] T. Plehn, M. Spannowsky, M. Takeuchi, [arXiv:1102.0557 [hep-ph]].
- [43] T. M. P. Tait and C. P. P. Yuan, Phys. Rev. D **63**, 014018 (2000) [arXiv:hep-ph/0007298].
- [44] K. Kondo, J. Phys. Soc. Jap. **57**, 4126-4140 (1988); K. Kondo, J. Phys. Soc. Jap. **60**, 836-844 (1991); F. Fiedler, A. Grohsjean, P. Haefner, P. Schieferdecker, Nucl. Instrum. Meth. **A624**, 203-218 (2010). [arXiv:1003.1316 [hep-ex]].
- [45] V. Barger, P. Huang, [arXiv:1102.3183 [hep-ph]].
- [46] The ATLAS Collaboration, G. Aad *et al.*, *Expected Performance of the ATLAS Experiment - Detector, Trigger and Physics*, arXiv: 0901.0512; E. Cogneras and D. Pallin, *Generic $t\bar{t}$ Resonance Search with the ATLAS Detector*, ATLPHYS-PUB-2006-033 (2006).
- [47] A. Abdesselam, E. B. Kuutmann, U. Bitenc *et al.*, [arXiv:1012.5412 [hep-ph]].
- [48] The ATLAS Collaboration, "Prospects for early $t\bar{t}$ resonance searches in ATLAS" (2010), ATL-PHYS-PUB-2010-008.
- [49] D. E. Kaplan, K. Rehermann, M. D. Schwartz and B. Tweedie, Phys. Rev. Lett. **101**, 142001 (2008) [arXiv:0806.0848 [hep-ph]].
- [50] J. Thaler, L. -T. Wang, JHEP **0807**, 092 (2008). [arXiv:0806.0023 [hep-ph]]; L. G. Almeida, S. J. Lee, G. Perez, G. F. Sterman, I. Sung, J. Virzi, Phys. Rev. **D79**, 074017 (2009).

- [arXiv:0807.0234 [hep-ph]]; J. M. Butterworth, A. R. Davison, M. Rubin, G. P. Salam, Phys. Rev. Lett. **100**, 242001 (2008). [arXiv:0802.2470 [hep-ph]].
- [51] H. Davoudiasl, J. L. Hewett, T. G. Rizzo, Phys. Rev. **D63**, 075004 (2001). [hep-ph/0006041].
- [52] J. L. Hewett, T. G. Rizzo, Phys. Rept. **183**, 193 (1989).
- [53] R. Frederix, F. Maltoni, JHEP **0901**, 047 (2009). [arXiv:0712.2355 [hep-ph]]; S. Moch, P. Uwer, Phys. Rev. **D78**, 034003 (2008). [arXiv:0804.1476 [hep-ph]].
- [54] V. Khachatryan *et al.* [CMS Collaboration], Phys. Rev. Lett. **105**, 211801 (2010). [arXiv:1010.0203 [hep-ex]].
- [55] H. Davoudiasl, J. L. Hewett, T. G. Rizzo, Phys. Rev. Lett. **84**, 2080 (2000). [hep-ph/9909255].
- [56] J. A. Aguilar-Saavedra, Nucl. Phys. **B843**, 638-672 (2011). [arXiv:1008.3562 [hep-ph]].
- [57] C. Zhang, S. Willenbrock, [arXiv:1008.3869 [hep-ph]].
- [58] C. Degrande, J. M. Gerard, C. Grojean, F. Maltoni and G. Servant, arXiv:1010.6304 [hep-ph].
- [59] B. Lillie, J. Shu and T. M. P. Tait, JHEP **0804**, 087 (2008) [arXiv:0712.3057 [hep-ph]]; K. Kumar, T. M. P. Tait and R. Vega-Morales, JHEP **0905**, 022 (2009) [arXiv:0901.3808 [hep-ph]].
- [60] D. Atwood, A. Kagan and T. G. Rizzo, Phys. Rev. D **52**, 6264 (1995) [arXiv:hep-ph/9407408].
- [61] The CMS Collaboration, “Measurement of the charge asymmetry in top quark pair production with the CMS experiment” (2011), CMS PAS TOP-10-010.